RSC Advances

PAPER

View Article Online
View Journal | View Issue

Cite this: *RSC Adv.*, 2021, **11**, 16955

Synthesis of 4-substituted catechols with side-chains of different C=C bond number as urushiol analogues and their anticorrosion performance†

Zeng-Feng Wei, *[a] Li-Jie Ni,[a] Heng Quan[a] and Jiang Duan*[b]

Received 13th February 2021
Accepted 27th April 2021

DOI: 10.1039/d1ra01195b

rsc.li/rsc-advances

4-Substituted catechols with different C=C bonds as urushiol analogues were synthesized through the a three-step route including reductive amination reaction of 3,4-dihydroxybenzaldehyde with *N*-Boc-piperazine, Boc deprotection, and amidation with various fatty acids. Electrochemical polymerization of these analogues on a copper surface afforded robust coatings with desirable adhesive force, hydrophobicity and thermal stability. Cyclic voltammetry and infrared spectroscopic characterizations revealed that the coating formation of urushiol analogues resulted from the electrooxidation-induced radical coupling of phenoxyl radicals with a phenyl ring and the side chain C=C bond. The coating of the urushiol analogue bearing only one side chain C=C bond exhibited the best performance in copper corrosion inhibition, with an inhibition efficiency of 99.99% and long-term effect (99.9% after 4 weeks of immersion in 3.5 wt% NaCl). The desired performance of these urushiol analogues suggests that they could be of practical applications as an alternative to the resource-limited natural urushiol.

Introduction

Among various metals, copper was the earliest and is the most widely used nonferrous metal; it is utilised in electrical engineering and other sectors because of its excellent thermal stability, electrical conductivity and mechanical properties and its relative inertness.[1–3] Although copper is relatively resistant to corrosion, it can be easily corroded in aggressive environments, such as sea water or acid solutions.[4,5] Owing to their low density, easy preparation, and excellent corrosion resistance and mechanical properties, organic coatings can effectively protect copper from corrosion.[6] However, organic coatings are eventually and gradually destroyed, leading to the formation of cracks and defects, resulting in coating failure.[7]

Raw lacquer is a natural resin that has been used in China for thousands of years because of its desirable coating properties, such as corrosion resistance, glossiness, solvent resistance, and thermal stability.[8] Urushiol, the main component and the major film-forming constituent of raw lacquer that accounts for 80–86 wt%,[9] is a mixture of 3-alkenylcatechols bearing C15 chains with 0–3 C=C bond(s).[10] However, its application is limited by scarce resources, low production and high costs.[11] Therefore, new strategies for synthesising urushiol analogues must be developed. Zhou *et al.*[12] obtained urushiol analogues by a one-step Friedel–Crafts alkylation reaction of methyl eleostearate (the main component of tung oil) with catechol *via* ultraviolet photocatalysis. Watanabe *et al.*[13] used eugenol (4-allyl-2-methoxyphenol) as a starting material and reacted it by organosilane protection, thiol–ene click reaction and deprotection to obtain several urushiol analogues with different alkyl chains. Although various synthetic methods for preparing urushiol analogues have been developed, a more economical method should be devised to achieve urushiol-like performance.

Drawing inspiration from the adhesive nature of catechols and amines in mussel adhesive proteins, researchers use polydopamine (PDA) as one of the most versatile approaches for functionalising almost all substrate surfaces.[14] PDA coatings can be formed in alkaline solutions without the need for any external conditions, such as light or heat, and can exhibit excellent adhesion capacities in aqueous environments.[15] Dopamine is a 4-substituted catechol derivative, and urushiol is actually a mixture of 3-alkenylcatechols. Therefore, we combined dopamine to construct urushiol analogues with 4-substituted catechol structure to improve coating adhesion. This beneficial property is more conducive to the long-term corrosion resistance of coatings under marine environments.

A previous study synthesised 3-substituted catechol at a medium yield *via* a two-step procedure, namely, Mannich reaction of catechol with formaldehyde and *N*-Boc-piperazine and deprotection, and amidation with various fatty acids.[16] In the present work, we directly introduced 4-substituted catechol

[a]*Hubei Provincial Key Laboratory of Biomass Fiber and Eco-Dyeing & Finishing, College of Chemistry & Chemical Engineering, Wuhan Textile University, Wuhan 430200, China. E-mail: zfwei@wtu.edu.cn*

[b]*Key Laboratory of Pesticide & Chemical Biology of the Ministry of Education, College of Chemistry, Central China Normal University, Wuhan 430079, P. R. China*

† Electronic supplementary information (ESI) available. See DOI: 10.1039/d1ra01195b

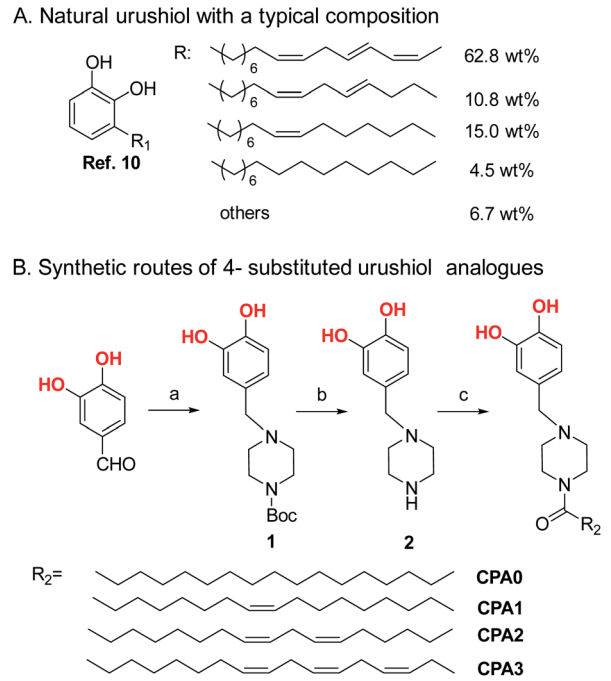

Scheme 1 Structure of natural urushiol (A) and synthetic routes of 4-substituted urushiol analogues (B). Reaction conditions: (a) *N*-Boc-piperazine, CH_3OH, 40 °C, 4 h; $NaBH_3CN$, 24 h. (b) HCl, ethyl acetate, r.t, 4 h. (c) R–COOH, NHS, EDC·HCl, CH_3OH, r.t, 12 h.

groups and further functionalised amine groups through the reductive amination reaction of 3,4-dihydroxybenzaldehyde and *N*-Boc-piperazine. Subsequently, we synthesised four 4-substituted catechols with different side chain saturations as urushiol analogues through deprotection and amidation reactions with different unsaturated fatty acids (Scheme 1). We examined the structures, morphologies and anticorrosion performance of cured coating and evaluated the structural effects of these properties. Results demonstrated that these urushiol analogues and their urushiol-like mixtures have the ability to form strong and thermally stable coatings with excellent corrosion inhibition performance. The raw materials are cheap and the synthesis of urushiol analogues can be produced on a large scale to reduce the cost. This is of great significance to the development of urushiol.

Results and discussion

Synthesis and characterization of urushiol analogues

The structures of CPA0–3 were characterised well by the ^{1}H NMR spectra (Fig. 1). Identical aromatic resonances appeared as a set of three signals of neighbouring three Ar–Hs with a 1 : 2 : 2 splitting pattern in δ 6.5–7.0 ppm, representing the 4-substituted catechol units of CPA0–3.[17] The differences in the CPA0–3 spectra according to the signals of the C=C bonds in the side chains, such as CPA0 has no but CPA1–3 have the vinylic hydrogen signal at δ 5.35 ppm, which increased in intensity with the increase in C=C bond numbers (marked in red in Fig. 1a). Another difference was that CPA2 and 3 showed the resonance of 1 and 2 methylene groups (marked in blue in Fig. 1b) flanked by two C=C bonds at δ 2.77 ppm. By contrast, CPA0 and CPA1 had no resonance. Moreover, both CPA1 and 3 displayed the C=C bond-neighbouring methylene absorption at 2.04 ppm (marked in purple Fig. 1c). The other similar characteristic resonances between CPA0 and 3 were the peaks of the linking methylene (N–CH_2) at 3.61 ppm, piperazine ring methylenes at 3.44 and 2.45 ppm, acyl methylene at 2.32 ppm and its next group at 1.62 ppm and other methylenes in the chain at ~1.27 ppm. The terminal –CH_3 of CPA0–2 appeared at δ 0.89 ppm, whereas it was absorbed at δ 0.98 ppm for CPA3.

The FTIR spectra of CPA0–3 showed no notable differences in terms of functional groups, except for the signals of the C=C bond in the side chains. As shown in Fig. 2, the catecholic hydroxyls of CPA0–3 were absorbed at 3250 cm^{-1} as a broad peak. The vinylic C–H bond stretched at 3013 cm^{-1}, with its intensity increasing with the increase in C=C bond numbers in the side chain. A strong saturated C–H absorption was observed at about 2800–2980 cm^{-1}. The amide group appeared intensively at 1607 cm^{-1}, phenyl ring band at about 1438 cm^{-1} and the phenylic O–H bending at ~1270 cm^{-1}.[18] The intensity of vinylic C–H bond could be an important indicator of their electropolymerisation reaction.

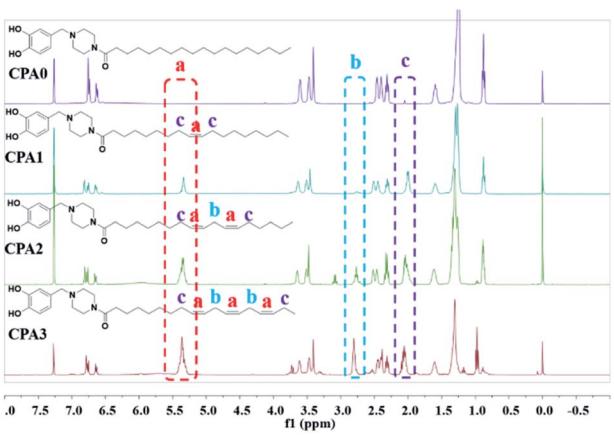

Fig. 1 Stacked ^{1}H NMR spectra of CPA0–3 for structural comparative analysis.

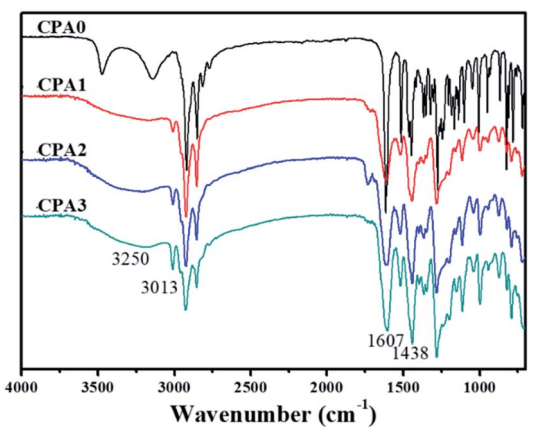

Fig. 2 FTIR spectra of CPA0–3.

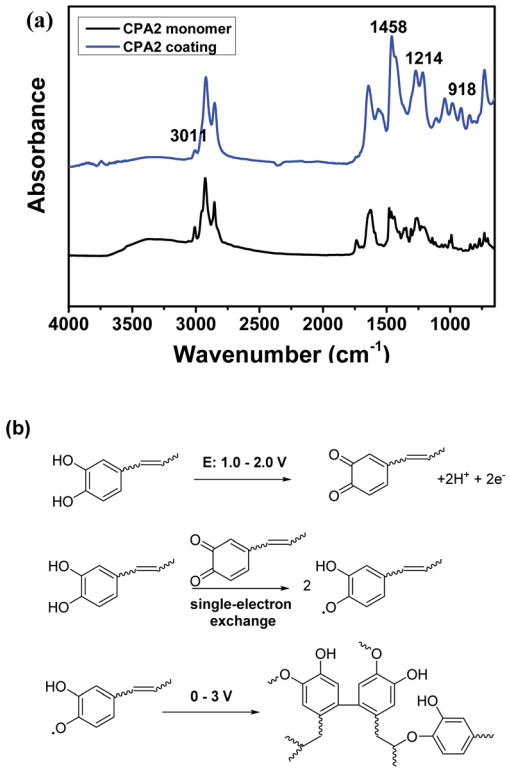

Fig. 3 The first scan of cyclic voltammetry plots of urushiol, CPA0–3 and CPAm in range of 0–3.0 V *vs.* SCE at scan rate 30 mV s^{-1} (a), and cyclic voltammetry plots of CPA3 with successive 15 potential scan cycles (b).

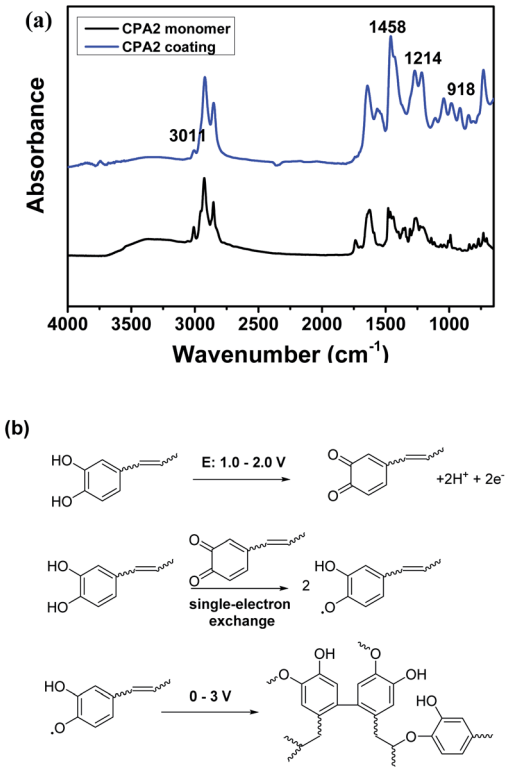

Fig. 4 ATR-FTIR spectra of CPA2 monomer and its coating (a), and the plausible electropolymerization mechanism of urushiol analogues (b).

Electropolymerization and its mechanism

CPA0–3 and CPAm were polymerised on the copper surface *via* cyclic voltammetry. As shown in Fig. 3a, an irreversible and broad oxidation peak between 0.7–1.5 V was found for urushiol, CPA0–3 and CPAm during the first scan cycle, which was attributed to catechol oxidation.[19] As scan number increased, the oxidation currents rapidly dropped and then remained constant (Fig. 3b), suggesting that the insulating coating formed on the copper surface.

The polymerisation of CPA0–3 and urushiol was also investigated by comparing the ATR-FTIR spectra before and after polymerisation (Fig. 4a and S1†). The spectra of the CPA2 monomer exhibited the characteristic broad phenolic O–H stretching absorption at about 3250 cm^{-1}, Ar–H and alkenyl ═C–H stretching at 3013 cm^{-1} and phenylic O–H bending at ~1270 cm^{-1}. After polymerisation, these characteristic absorption peaks showed several differences. A remarkable decrease in ═C–H stretching was observed at 3011 cm^{-1}, which could be attributed to the participation of C═C bonds in the polymerisation. Moreover, the phenyl ring band was enhanced at about 1458–1560 cm^{-1} due to the coupling of phenyl rings. Furthermore, the appearance of new adsorptions at about 1214 and 918 cm^{-1} was ascribed to the formation of aromatic ether bonds and *trans* C═C bonds, respectively, during polymerisation.[20]

The results of cyclic voltammetry and ATR-FTIR combined with the possible mechanisms of urushiol according to different methods[16,21,22] suggested that the electropolymerisation of the analogues was an electrochemically initiated radical polymerisation process on the copper surface (Fig. 4b). First, the catechol unit in the analogues was anodically oxidised to quinone form within 0.7–1.5 V. Second, the quinone immediately reacted with another catechol unit to form semiquinone radical species *via* a single-electron exchange process.[23] Finally, several radical couplings occurred between the phenoxyl radical with phenyl ring and the C═C bonds in the side chains, leading to the formation of a complex crosslinking network.

Coating properties

The coating thickness, hardness, adhesion strength, water contact angle and thermal stability of the electropolymerised coatings were also investigated (Table 1). The coating thicknesses of CPA0–3, as well as of CPAm, were between 11.2 and 14.6 μm. However, the coating of urushiol was only 7.5 μm thick, indicating that the urushiol analogues underwent crosslinking reaction at a similar rate during the electropolymerisation process and were faster than urushiol. By comparison, their coating hardness varied from 1H to 6H, and all coatings were hydrophobic with water contact angles ranging from 95.5° to 107.2°. The highest hardness of the urushiol coating was 6H, whereas those of the coatings of urushiol analogues displayed a moderate hardness of 1–2H, suggesting that the number of C═C bonds in the side chains did not affect coating hardness. The adhesion strength of the coatings was

Table 1 Physical properties and thermal stability of the electropolymerization coatings

Coating	Thickness (μm)	Pencil hardness	Adhesion strength	Contact angle (°)	$T_{10\%}$ (°C)	$T_{50\%}$ (°C)	T_{max} (°C)	W_{char} (%)
CPA0	11.2 ± 1.9	2H	5B	106.2 ± 1.0	268.7	428.8	421.6	27.50
CPA1	14.6 ± 1.1	1H	4B	95.5 ± 1.1	244.6	437.8	425.6	29.84
CPA2	12.7 ± 1.8	1H	2B	98.3 ± 1.6	238.9	444.7	411.9	40.68
CPA3	14.5 ± 3.4	1H	3B	107.2 ± 2.7	250.6	479.4	420.7	46.09
CPAm	12.8 ± 2.7	2H	3B	104.5 ± 4.8	262.6	540.5	446.9	46.48
Urushiol	7.5 ± 1.3	6H	5B	98.5 ± 1.1	321.8	446.5	437.2	34.62

also measured. The adhesion strength of CPA0, CPA1, CPA2, CPA3 and urushiol coating was 5B, 4B, 2B, 3B, 3B and 5B, respectively. However, the adhesion force of urushiol analogue coatings was worse than that of natural urushiol (which exhibited an excellent adhesion strength of 5B), suggesting that the substitution position had a considerable impact on coating adhesion performance. Moreover, the 3-substituted catechol structure was more conducive than 4-substituted in terms of adhesion onto the copper substrates probably because the adhesion of dopamine not only came from the 4-substituted catechol structure but also from the amino group. By contrast, urushiol coating had excellent durability, and its main composition is 3-alkenylcatechols,[24] illustrating that if the side chain was long, then the 3-substituted catechol structure was beneficial to adhesion capacity.

Thermal stability, which was measured *via* TGA, is another important factor of coatings (Fig. 5). Thermal stability includes weight loss temperatures ($T_{10\%}$ and $T_{50\%}$), maximum weight loss rate (T_{max}) and char yield at 600 °C (W_{char}) (Table 1). All coatings exhibited a three-step thermal degradation process. The first step degradation occurred at about 100–150 °C and corresponded to the evaporation of water. The second step, which occurred within the range of 220–330 °C, was the thermal degradation of unreacted C=C bonds or oligomers. The third (and the fastest) degradation step occurred at about 330–480 °C, which was attributed to the decomposition of the polymers. All individual coatings of the analogues and their mixtures had similar $T_{10\%}$ values ranging from 238.9 °C to 268.4 °C, which were obviously inferior to that of urushiol (321.8 °C). CPA0–3 had $T_{50\%}$ values ranging from 428.8 °C to 479.4 °C, similar to that of urushiol. All the T_{max} values for the analogues were about 420 °C, which was slightly lower than that of urushiol (437.2 °C). This was not the case for CPAm coating, which had the highest $T_{50\%}$ (540.5 °C), T_{max} (446.9 °C) and W_{char} values (46.48%). The W_{char} values increased as the number of C=C bonds increased, which was ascribed to the formation of a higher degree of cross-linking network with a higher content of C=C bonds in the side chains. The results of TG analysis demonstrated that these analogues and their mixtures have a high thermal stability.

SEM images of the surfaces of the electropolymerised coatings are shown in Fig. 6. The CPA0 surface had a rough and uneven surface. As the number of C=C bonds increased, the surfaces of the CAP1–3 coatings became smoother and flat, demonstrating a higher degree of cross-linking network. Moreover, some particles appeared on the coatings' surfaces possibly because of the polymerisation of urushiol analogues in the solution and the formation of nanoscale particles that attached onto the coatings' surfaces. Furthermore, compared to the surface of CPA2 and CPA3, the surface of the CPA1 coating had an obviously aggregated morphology, which was more close to that of natural urushiol coatings, indicating that CPA1 may have film-forming properties similar to those of natural urushiol.

Anticorrosion performance

The electrochemical experiments of urushiol analogue coatings were investigated to determine their corrosion protection performance relative to that of urushiol. Corrosion inhibition behaviour was examined *via* potentiodynamic polarisation (Fig. 7). Values of corrosion current density (i_{corr}) and potential

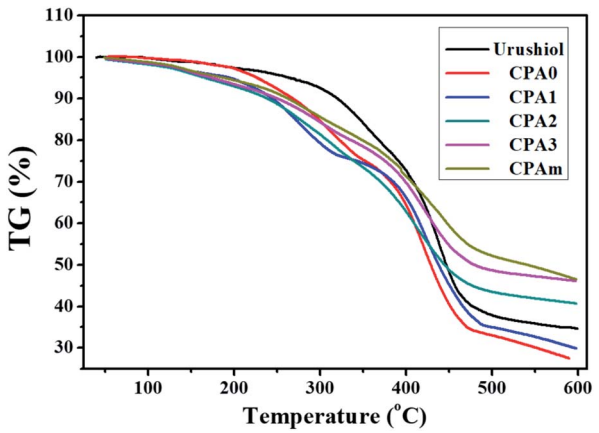

Fig. 5 TG analysis of the coatings of urushiol and urushiol analogues.

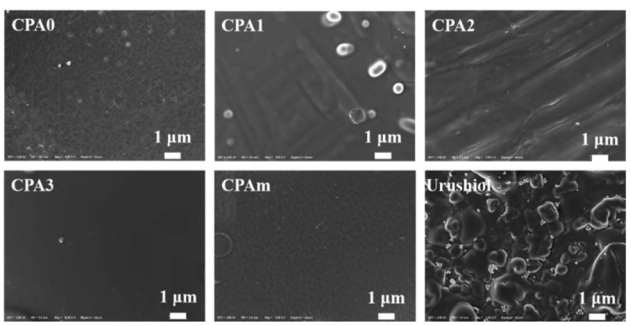

Fig. 6 SEM photographs of different electro-polymerization coatings.

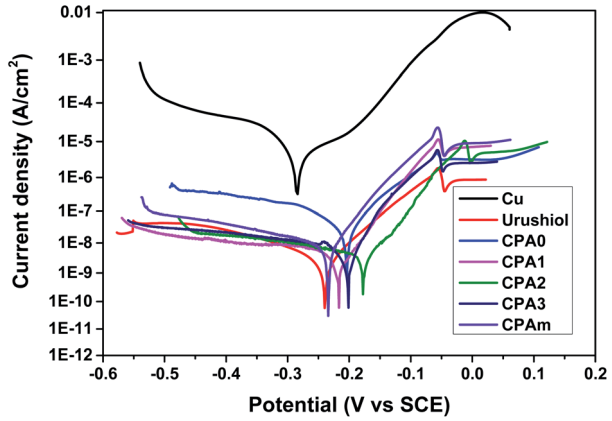

Fig. 7 Polarization curves for copper, urushiol and urushiol analogues coating in 3.5 wt% NaCl solution at 25 °C.

(E_{corr}), along with the estimated corrosion rate (CR) and IE, are summarised in Table 2.

Regardless of the type of coating, i_{corr} substantially decreased by 3 to 4 orders of magnitude. Moreover, E_{corr} shifted to a high positive potential compared with the copper substrate. The CPA0 coating showed a slightly larger i_{corr} (3.30×10^{-8}) than the other coatings, which exhibited similar i_{corr} values in the order of 10^{-9}. Furthermore, these coatings were estimated to have corrosion rates ranging from 10^{-4} to 10^{-5} mm per year, considerably lower than that of bare copper.[16] Calculation of the i_{corr} and CR values of CPA0–3, CPAm and urushiol coatings achieved excellent IE values ranging from 99.85% to 99.99%. The CPA1 and CPA2 coatings exhibited an anticorrosion performance similar to that of natural urushiol.

The Nyquist plots of EIS measurements for copper, urushiol and urushiol analogue coatings in 3.5 wt% NaCl solution at 25 °C are presented in Fig. 8a. Values of solvent resistance (R_s), charge transfer resistance (R_{ct}) and coating resistance (R_c) were obtained by fitting the impedance data to the equivalent circuit models (Fig. 8b). The Nyquist diagram of the urushiol analogue coatings did not have one but two capacitive arcs,[25] indicating that two RC parallel circuits were present on the copper surface. Meanwhile, the total resistance of the coatings (R_p) was calculated as follows:[26]

$$1/R_p = 1/(R_c + R_{ct}) \quad (1)$$

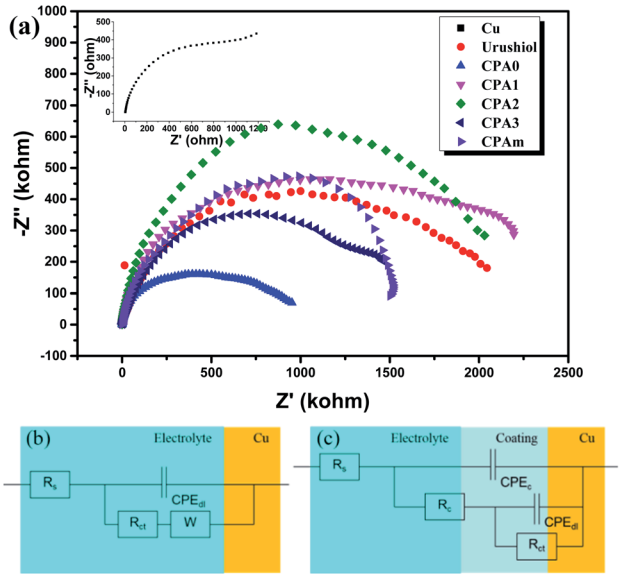

Fig. 8 Nyquist polts for copper, urushiol and urushiol analogues coating in 3.5 wt% NaCl solution at 25 °C (a) and equivalent circuit model used for fitting EIS dates of bare Cu (b) and coated Cu (c).

The R_p values are summarised in Table 2. The R_p of copper, urushiol, CPA0–3 and CPAm was 1.66×10^3, 2.30×10^6, 1.06×10^6, 2.27×10^6, 2.18×10^6, 1.53×10^6 and 1.53×10^6 Ω cm^2, respectively. Compared with that of bare copper, the R_p of all coatings remarkably decreased, indicating excellent corrosion resistance. The CPA1 and CPA2 coatings exhibited superior performance, consistent with the results of potentiodynamic polarisation characterisation, thereby confirming the reliability of anticorrosion performance.

The long-term corrosion inhibition of the CPA0–3 and CPAm coatings on copper was also tested *via* potentiodynamic polarisation and compared with that of urushiol coating (Fig. 9). During the first 2 weeks, the IE of the coatings begun to decrease but remained higher than 99%, except for CPA2 (98%). When the coatings were immersed for 4 weeks, their IE values were still higher than 93%, especially for CPA1, which maintained IE values of >99%, which was even higher than that of the natural urushiol coating. This desirable anticorrosion performance and durability were attributed to the uniform structure and the multiple-crosslinking networks of the urushiol analogues that prevented the contact of copper with the corrosive species.[27] Notably, the long-term corrosion inhibition

Table 2 Corrosion data of copper with and without coating

Sample	i_{corr} (A cm^{-2})	E_{corr} (V *vs.* SCE)	CR (mm per year)	IE (%)	R_p (Ω cm^2)
Copper	2.23×10^{-5}	−0.283	2.59×10^{-1}	—	1.66×10^3
Urushiol	2.50×10^{-9}	−0.208	2.90×10^{-5}	99.99	2.30×10^6
CPA0	3.30×10^{-8}	−0.204	3.83×10^{-4}	99.85	1.06×10^6
CPA1	2.73×10^{-9}	−0.216	3.17×10^{-5}	99.99	2.27×10^6
CPA2	3.12×10^{-9}	−0.176	2.47×10^{-5}	99.99	2.18×10^6
CPA3	7.24×10^{-9}	−0.203	8.39×10^{-5}	99.97	1.53×10^6
CPAm	9.34×10^{-9}	−0.235	1.08×10^{-4}	99.96	1.53×10^6

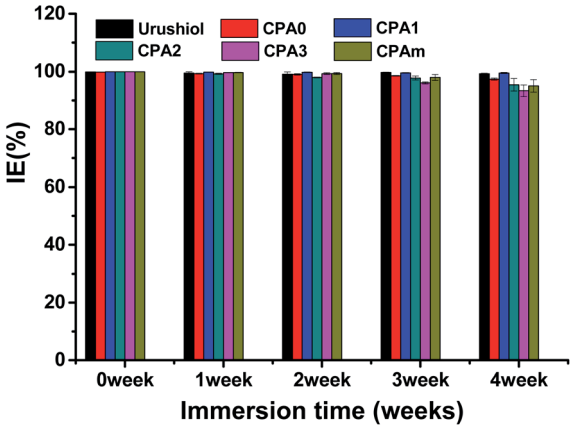

Fig. 9 Bar graph of the long-term corrosion resistance of urushiol and its analogue coatings.

effects of these coatings were comparable to those of a recently reported urushiol or lacquer coating[26,28] but inferior to those of urushiol analogue coatings with a 3-substituted structure.[16] Therefore, the substitution position on the catechol not only affected the adhesion capability but also the anticorrosion performance of the urushiol analogues.

Conclusions

In this work, 4-substituted catechols with side-chains of different C=C bond numbers as urushiol analogues were designed and synthesised, and their anticorrosion performance on copper was investigated. This synthetic method conveniently obtained the urushiol analogues as alternatives of resource-limited natural urushiol with a high yield. The analogue coatings exhibited excellent and long-term corrosion inhibition performance on copper, which was attributed to the formation of a complex cross-linking network by electropolymerisation. The urushiol analogue with one C=C bond in the side chain displayed the best anticorrosion performance, even better than that of natural urushiol. This study determined the effects of the content of double bonds on the performance of urushiol analogues. It provides guidelines for the design of urushiol analogues.

Experimental

Materials

Raw lacquer was provided by the Institute of Lacquer (Xi'an, China). Urushiol (98%) was extracted from the raw lacquer by using ethanol following a previously described method.[29] *N*-Boc-piperazine, oleic acid (98%), α-linolenic acid (85%) and linoleic acid (98%) were purchased from Aladdin Reagent Co., Ltd. (China). 3,4-Dihydroxybenzaldehyde, 1-ethyl-3-(3-dimethylaminopropyl) carbodiimide hydrochloride, $NaBH_3CN$, *N*-hydroxysuccinimide and stearic acid were acquired from Sinopharm Chemical Reagents Co., Ltd. (China). Other reagents and solvents were of analytical grade and used without further purification.

Synthesis and characterization of urushiol analogues

As shown in Scheme 1B, 4-substituted catechols were synthesised *via* a two-step procedure. These urushiol analogues bearing 0–3 C=C bonds in the side chains were correspondingly named as CPA0 (81% yield), CPA1 (78% yield), CPA2 (78% yield), and CPA3 (75% yield). The mixture consisting of CPA0 (4.5 wt%), CPA1 (15.0 wt%), CPA2 (10.8 wt%) and CPA3 (62.8 wt%) was denoted as CPAm according to the typical content of natural urushiol. The structures of these urushiol analogues were characterised *via* ^{1}H NMR, ^{13}C NMR, FTIR, and HRMS. NMR spectra were recorded on a Varian NMR spectrometer (Mercury plus-400) by using $CDCl_3$ as the solvent. Chemical shifts were reported in terms of parts per million (ppm) relative to tetramethylsilane. High-resolution ESI mass spectra were obtained on an Agilent 6530 accurate-mass Q-TOF spectrometer. FTIR spectra were measured by Burker Tensor 27 infrared spectrometer. The details are described in ESI.†

Coating preparation

Copper foils (>99.7%) were polished with emery papers of different grades, cut into square pieces with a dimension of 15.0 mm × 10.0 mm × 1.0 mm, ultrasonicated with ethanol for 5 min, and then blown-dried. The urushiol analogue coatings were formed on the copper foils *via* cyclic voltammetry with potential sweeping from 0–3 V *vs.* saturated calomel electrode (SCE) at a rate of 30 mV s^{-1} for 15 cycles through Autolab PGSTAT30 (Echo Chemie B.V., the Netherlands), with an SCE as the reference electrode and a platinum plate as the counter electrode. The electrolyte was 30 mg mL^{-1} urushiol or urushiol analogue in 1 mM Tris–HCl (pH 8.5) ethanol/water solution (10 : 1 in volume).

Characterization of coating

Attenuated total reflection (ATR)-FTIR was measured using a Nicolet iS10 spectrometer (Thermo Scientific, USA). Coating thickness was measured by a coating thickness gauge (EC-770, Yuwese, China). The adhesion force of the coatings was investigated according to ASTM D3359 method, and pencil hardness was determined by the standard test method ASTM D3363. Static contact angle (3 μL water) was measured using a contact angle system (OCA 20, Dataphysics, Germany) and repeated to five times on different spots. The coating thermal stability was investigated *via* thermogravimetric analysis (TGA 4000, Perkin Elmer, USA) at a heating rate of 10 °C min^{-1} under N_2 atmosphere. The surface morphologies of the substrates were acquired using a Zeiss Ultra Plus field-emission scanning electron microscope (SEM) (Carl Zeiss AG, Germany) with an accelerating voltage of 15 kV.

Electrochemical corrosion measurement

Electrochemical measurements were performed in 3.5 wt% NaCl solution by potentiodynamic polarisation and electrochemical impedance spectroscopy (EIS).[30] Potentiodynamic polarisation tests were conducted from ±300 mV *vs.* steady open circuit potential at a rate of 1 mV s^{-1} and 25 °C. The EIS

was measured within the 10^{-2} to 10^{5} Hz frequency range with applied 10 mV sinusoidal perturbations. Each measurement was measured three times to ensure reproducibility. Inhibition efficiency (IE) was calculated as follows:

$$\mathrm{IE}\ (\%) = (i_{\mathrm{corr}(0)} - i_{\mathrm{corr}(c)})/i_{\mathrm{corr}(0)} \times 100 \quad (2)$$

where $i_{\mathrm{corr}(0)}$ and $i_{\mathrm{corr}(c)}$ are the corrosion current densities in the absence and the presence of coatings, respectively. Corrosion rate (CR) was calculated as follows:

$$\mathrm{CR} = K(i_{\mathrm{corr}}/\rho)E_{\mathrm{w}} \quad (3)$$

where K is a conversion constant (3.27×10^{-3} mm g per μA cm year),[31] ρ (= 8.96 g cm^{-3}) is the density of copper, and E_{w} (= 31.77) is the equivalent weight of copper.

Conflicts of interest

There are no conflicts to declare.

Acknowledgements

The authors gratefully acknowledge the financial supports from the National Natural Science Foundation of China (21905104), the Wuhan Municipal Front Program for Application Basis Research (2018010401011283), and the Open Project of Hubei Provincial Key Laboratory of Biomass Fiber and Eco-Dyeing & Finishing (STRZ2020034).

Notes and references

1 Y. Zeng, Z. Qin, Q. Hua, Y. Min and Q. Xu, *Surf. Coat. Technol.*, 2019, **362**, 62–71.
2 V. Maurice, A. Seyeux, L. H. Klein, E. Salmi, M. Ritala and P. Marcus, *Appl. Surf. Sci.*, 2016, **387**, 1054–1061.
3 T. Liu, S. Chen, S. Cheng, J. Tian, X. Chang and Y. Yin, *Electrochim. Acta*, 2007, **52**, 8003–8007.
4 Z. Lu, P. Wang and D. Zhang, *Corros. Sci.*, 2015, **91**, 287–296.
5 W. Liu, Q. Xu, J. Han, X. Chen and Y. Min, *Corros. Sci.*, 2016, **110**, 105–113.
6 M. Bahrami, Z. Ranjbar, R. A. Khosroshahi and S. Ashhari, *Prog. Org. Coatings*, 2017, **113**, 25–30.
7 J. Wei, B. Li, L. Jing, N. Tian, X. Zhao and J. Zhang, *Chem. Eng. J.*, 2020, **390**, 124562.
8 J. Yang, N. Chen, J. Zhu, J. Cai, J. Deng, F. Pan, L. Gao, Z. Jiang and F. Shen, *Sci. Rep.*, 2020, **10**, 1–9.
9 T. Honda, R. Lu and T. Miyakoshi, *Prog. Org. Coat.*, 2006, **56**, 279–284.
10 Y. Fang, L. Yan and H. Liu, *ACS Appl. Polym. Mater.*, 2020, **2**, 3781–3788.
11 H. Je and J. Won, *Chem. Eng. J.*, 2021, **404**, 126424.
12 C. Zhou, Y. Hu, Z. Yang, T. Yuan, J. Huang, P. Li, Y. Liu, S. Zhang and Z. Yang, *Prog. Org. Coat.*, 2018, **120**, 240–251.
13 H. Watanabe, M. Takahashi, H. Kihara and M. Yoshida, *ACS Appl. Bio Mater.*, 2018, **1**, 808–813.
14 Y. Zou, X. Chen, P. Yang, G. Liang, Y. Yang, Z. Gu and Y. Li, *Sci. Adv.*, 2020, **6**, 1–10.
15 J. Saiz-Poseu, J. Mancebo-Aracil, F. Nador, F. Busqué and D. Ruiz-Molina, *Angew. Chem., Int. Ed.*, 2019, **131**, 706–725.
16 Z. Wei, X. Chen, J. Duan, C. Mei, D. Xiao and A. Zhang, *RSC Adv.*, 2019, **9**, 24904–24914.
17 J. Duan, W. Wu, Z. Wei, D. Zhu, H. Tu and A. Zhang, *Green Chem.*, 2018, **20**, 912–920.
18 L. Zheng, Y. Lin, D. Wang, J. Chen, K. Yang, B. Zheng, W. Bai, R. Jian and Y. Xu, *RSC Adv.*, 2020, **10**, 13936–13943.
19 D. Rojas, F. Della Pelle, M. Del Carlo, D. Compagnone and A. Escarpa, *Electrochem. Commun.*, 2020, **115**, 106718.
20 N. Lone, I. W. Cheong, M. Cho, Y. K. Hong, Y. S. Choi, S. Perumal, B. T. Oh and J. Joo, *J. Coatings Technol. Res.*, 2017, **14**, 621–630.
21 M. Ko, J. Jung, S. S. Hwang and J. Won, *Polymer*, 2020, **205**, 122835.
22 S. Kobayashi, *Struct. Chem.*, 2017, **28**, 461–474.
23 C. Zhang, M. Ma, T. Chen, H. Zhang, D. Hu, B. Wu, J. Ji and Z. Xu, *ACS Appl. Mater. Interfaces*, 2015, **9**, 34356–34366.
24 D. Tamburini, I. Bonaduce and M. P. Colombini, *J. Anal. Appl. Pyrolysis*, 2015, **116**, 129–141.
25 R. Fuchs-Godec and G. Zerjav, *Corros. Sci.*, 2015, **97**, 7–16.
26 F. Elmi, A. Gharakhani, S. Ghasemi and H. Alinezhad, *Prog. Org. Coat.*, 2018, **119**, 127–137.
27 H. Liu, B. Fan, G. Fan, Y. Ma, H. Hao and W. Zhang, *J. Mater. Sci. Technol.*, 2021, **72**, 202–216.
28 L. Zhang, H. Wu, Z. Zheng, H. He, M. Wei and X. Huang, *Prog. Org. Coat.*, 2019, **127**, 131–139.
29 X. Fan, W. Zhou, Y. Chen, L. Yan, Y. Fang and H. Liu, *ACS Appl. Mater. Interfaces*, 2020, **12**, 32031–32040.
30 Z. Wei, X. Chen, J. Duan, G. Zhan, Y. Wei and A. Zhang, *J. Mol. Liq.*, 2019, **280**, 327–333.
31 K. Akhtar, U. Hira, H. Khalid and N. Zubair, *J. Alloys Compd.*, 2019, **772**, 15–24.